

Isostaticity and the solidification of semiflexible polymer melts

Christian O. Plaza-Rivera, Hong T. Nguyen, and Robert S. Hoy*
Department of Physics, University of South Florida, Tampa, FL 33620, USA
 (Dated: September 8, 2021)

Using molecular dynamics simulations of a tangent-soft-sphere bead-spring polymer model, we examine the degree to which semiflexible polymer melts solidify at isostaticity. Flexible and stiff chains crystallize when they are isostatic as defined by appropriate degree-of-freedom-counting arguments. Semiflexible chains also solidify when isostatic if a generalized isostaticity criterion that accounts for the slow freezing out of configurational freedom as chain stiffness increases is employed. The dependence of the average coordination number at solidification $Z(T_s)$ on chains' characteristic ratio C_∞ has the same functional form [$Z \simeq a - b \ln(C_\infty)$] as the dependence of the average coordination number at jamming $Z(\phi_J)$ on C_∞ in athermal systems, suggesting that jamming-related phenomena play a significant role in thermal polymer solidification.

I. INTRODUCTION

Traditional analytic criteria for solidification, such as those based on classical nucleation theory, typically work very poorly both for liquids with strong glassforming tendency and for polymeric liquids. This failure creates a need for alternative criteria predicting these systems' solidification transitions. Several have been proposed, such as the splitting of the first peak in the pair correlation function $g(r)$, the height of this peak g_{max} and its ratio to the value g_{min} of $g(r)$ at its first minimum, and other criteria based on $g(r)$ or local, cluster-level structure.[1–6] Criteria based on the average coordination number $\langle Z \rangle$, such as the famous result that systems of spherical particles jam at isostaticity [$\langle Z \rangle = 2d$, where d is spatial dimension][7, 8] naturally fit into both of these categories.

Recent work[9–12] has suggested an interesting connection between isostaticity and solidification of polymeric liquids: that solidification occurs when the average number of noncovalent contacts per monomer $\langle Z_{nc} \rangle$ exceeds its isostatic value $\langle Z_{nc}^{iso} \rangle$. These studies focused on liquids of fully flexible[9–12] or infinitely stiff[12] chains, for which the definition of $\langle Z_{nc}^{iso} \rangle$ is straightforward. However, *finite* chain stiffness is well known to strongly and nontrivially affect polymer solidification in both thermal[13–15] and athermal[16, 17] systems. Here we examine the connection of isostaticity to polymer solidification using molecular dynamics simulations of a simple crystallizable bead-spring model[18] with continuously variable chain stiffness. By considering chains ranging from flexible to rodlike and employing a suitably generalized isostaticity criterion, we show that these model polymeric liquids are very generally isostatic at their solidification temperatures.

Consider $d = 3$ chains of length N with monomer positions \vec{r}_i , covalent bond lengths $\ell_i = |\vec{r}_{i+1} - \vec{r}_i|$, and bond angles $\theta_i = \cos^{-1}[\vec{\ell}_{i-1} \cdot \vec{\ell}_i / (\ell_{i-1} \ell_i)]$. Maxwell's isostaticity criterion[7] can be written as $\langle Z^{iso} \rangle = 2N^{-1}(Nd - n_{constr})$, where n_{constr} is the number of holonomic con-

straints per chain. Fixed-length ($\ell = \ell_0$) covalent bonds and fixed bond angles ($\theta = \theta_0$) respectively supply $N - 1$ and $N - 2$ constraints per chain.[19, 20] Fully flexible chains with fixed-length covalent bonds have[12]

$$\langle Z_{nc}^{iso} \rangle = \langle Z_{nc}^{iso} \rangle_{flex} = \frac{2[3N - (N - 1)]}{N} = 4 + \frac{2}{N}, \quad (1)$$

while infinitely stiff chains that also have fixed bond angles have[12]

$$\langle Z_{nc}^{iso} \rangle = \langle Z_{nc}^{iso} \rangle_{stiff} = \frac{2[3N - (N - 1) - (N - 2)]}{N} = 2 + \frac{6}{N}. \quad (2)$$

For semiflexible chains, a more general isostaticity criterion intermediate between Eqs. 1 and 2 may apply.[21] If isostaticity controls solidification but angular degrees of freedom are *gradually* frozen out as chain stiffness increases, the average number of noncovalent contacts per monomer at the solidification temperature T_s , $\langle Z_{nc}(T_s) \rangle$, should vary smoothly from $\langle Z_{nc}^{iso} \rangle_{flex}$ to $\langle Z_{nc}^{iso} \rangle_{stiff}$. Below, we use molecular dynamics simulations to show that this indeed occurs in model systems, and derive a generalized isostaticity criterion describing the phenomenon.

II. MODEL AND METHODS

Our simulations employ the soft-pearl-necklace polymer model described at length in Refs.[15, 18] It is comparable to the Kremer-Grest bead-spring model,[22] but possesses crystalline ground states. All monomers have mass m and interact via the truncated and shifted Lennard-Jones potential

$$U_{LJ}(r) = \epsilon \left[\left(\frac{\sigma}{r} \right)^{12} - \left(\frac{\sigma}{r_c} \right)^{12} - 2 \left(\left(\frac{\sigma}{r} \right)^6 - \left(\frac{\sigma}{r_c} \right)^6 \right) \right], \quad (3)$$

where ϵ is the intermonomer binding energy and $r_c = 2^{7/6}\sigma$ is the cutoff radius. Bonds between adjacent beads along the chain backbone are modeled using the harmonic potential

$$U_c(\ell) = \frac{k_c}{2} (\ell - \sigma)^2, \quad (4)$$

* rshoy@usf.edu

where ℓ is bond length and k_c is the bond stiffness. The large value of k_c employed here ($600\epsilon/\sigma^2$) produces bonds of nearly fixed ℓ ; $U_c(\ell)$ effectively acts as a holonomic constraint fixing $\ell = \ell_0 = \sigma$ and preventing chain crossing.[18] Bending stiffness is included using the standard potential[23]

$$U_b(\theta) = k_{bend}(1 - \cos(\theta)), \quad (5)$$

which favors straight trimers (sets the equilibrium bond angle $\theta_0 = 0$). Fully flexible chains have $k_{bend} = 0$, and rigid-rod-like chains are obtained in the limit $k_{bend} \rightarrow \infty$. Here we study systems with $0 \leq k_{bend} \leq 30\epsilon$. As detailed in Ref.[15], the model's solid morphologies – formed by cooling from the isotropic liquid state – range from random-walk close-packed crystals to glasses to nematic close-packed crystals over this range of k_{bend} . Since its solidification dynamics[24] also vary strongly with k_{bend} , the model is suitable for studying connections between solidification and isostaticity in a very general way.

All systems are composed of $N_{ch} = 500$ chains of $N = 25$ monomers. These chains are unentangled. Periodic boundaries are applied along all three directions of cubic simulation cells. Systems are first thoroughly equilibrated [23] at temperatures well above their k_{bend} -dependent solidification temperatures,[15] then slowly cooled at zero pressure to $T = 0$ at a rate $|\dot{T}| = 10^{-6}/\tau$. This $|\dot{T}|$ is sufficiently low to be in a limit where finite-cooling-rate effects on melt structure are small.[24] Pressure is controlled using a Nose-Hoover barostat. The MD timestep used here is $\delta t = \tau/200$, where τ is the Lennard-Jones time unit $\sqrt{m\sigma^2/\epsilon}$. All simulations are performed using LAMMPS.[25]

III. RESULTS

Ref.[15] presented a detailed analysis of these systems' solidification behavior for $k_{bend} \leq 12.5\epsilon$, but did not consider staticity. Figure 1 presents staticity-related results. Panel (a) shows how $\langle Z_{nc}(T) \rangle$ increases during cooling for four representative chain stiffnesses: flexible ($k_{bend} = 0$), semiflexible ($k_{bend} = 4\epsilon$), semistiff ($k_{bend} = 10\epsilon$), and stiff ($k_{bend} = 30\epsilon$). Here

$$\langle Z_{nc} \rangle = \frac{2}{N_{ch}N} \sum_{i=1}^{N_{ch}N} \sum_{j=i+1}^{N_{ch}N} \Theta(1 - r_{ij}) f_{ij}, \quad (6)$$

where $\Theta(x)$ is the Heaviside step function; $f_{ij} = 0$ if monomers i and j are covalently bonded and 1 otherwise. Thus $\langle Z_{nc} \rangle$ only counts *repulsively* interacting particles (those with $r_{ij} \equiv |\vec{r}_j - \vec{r}_i| < 1$) as being in contact, as is appropriate for thermal systems.[21] Flexible chains crystallize into a random-walk close-packed (RWCP) structure wherein monomers close-pack but chains retain random-walk-like structure and are isotropically oriented.[15] Semiflexible chains form

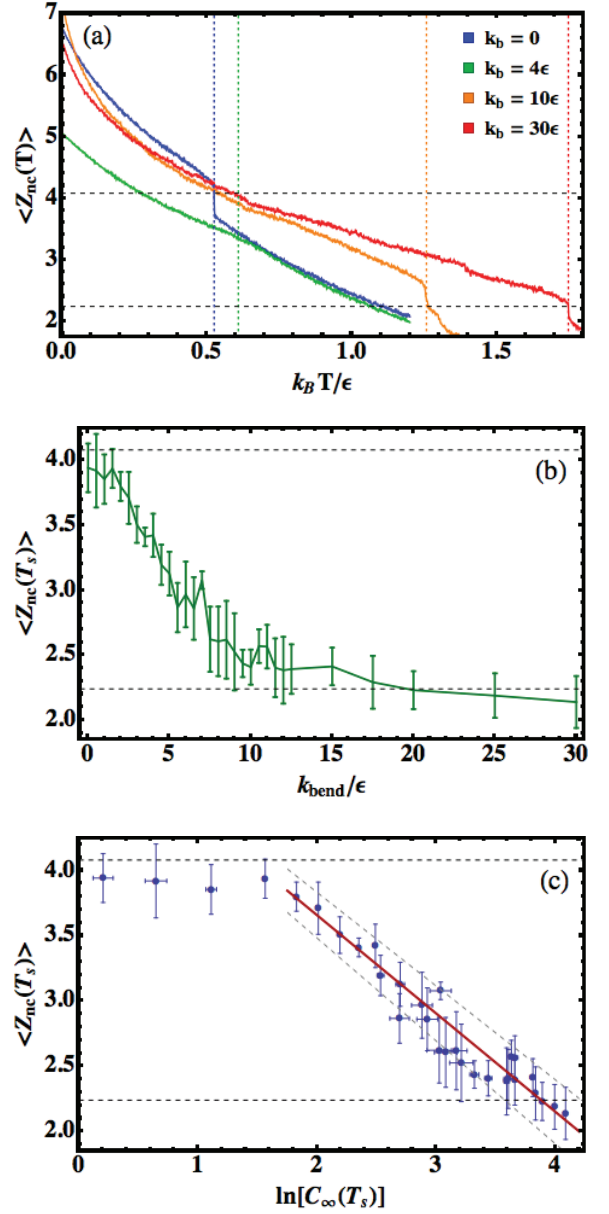


FIG. 1. Measures of noncovalent repulsive contacts in slowly cooled semiflexible polymer melts. Panel (a) shows $\langle Z_{nc}(T) \rangle$: blue, green, orange and red curves show data for selected k_{bend} , while the correspondingly colored vertical dotted lines indicate the respective $T_s(k_{bend})$ [Table I]. Panel (b) shows the k_{bend} -dependence of $\langle Z_{nc}(T_s) \rangle$ for all systems. In panel (c), points show the same $\langle Z_{nc}(T_s) \rangle$ as in panel (b), but plotted vs. $C_\infty(T_s)$. The red solid line shows a fit to our generalized isostaticity criterion (Eq. 9), and the angled dotted lines show the maximal statistical uncertainties on this fit, including uncertainties on both the slope b and the intercept $[\langle Z_{nc}^{iso} \rangle_{flex} - \langle Z_{nc}^{iso} \rangle_{stiff}] / b$. In all panels, the upper and lower horizontal gray dotted lines respectively indicate $\langle Z_{nc}^{iso} \rangle_{flex} = 4.08$ and $\langle Z_{nc}^{iso} \rangle_{stiff} = 2.24$ for these $N = 25$ systems. Results from separate studies of $N = 13$ and $N = 50$ systems for selected k_{bend} (not shown) were in all ways consistent with those shown here.

TABLE I. Solidification temperatures, densities, and solid morphologies for selected chain stiffnesses. Values of T_s and ϕ_s for $k_{bend} \leq 12.5\epsilon$ and morphology descriptions were reported in Ref.[15].

k_{bend}/ϵ	$k_B T_s/\epsilon$	ϕ_s	Morphology
0	0.53	0.684	RWCP
2	0.49	0.673	glass/RWCP
4	0.61	0.646	glass
6	0.91	0.606	nematic glass
8	1.13	0.581	multidomain NCP
10	1.26	0.580	defected NCP
15	1.32	0.582	NCP
20	1.57	0.558	NCP
25	1.66	0.556	NCP
30	1.75	0.552	NCP

glasses; $k_{bend} = 4\epsilon$ systems have been shown to be typical fragile glassformers.[24] Semistiff chains form moderately defective nematic close-packed (NCP) crystals,[15] while stiff chains form nearly perfect NCP crystals. Solidification temperatures T_s increase by more than a factor of three (from $k_B T_s/\epsilon = 0.53$ for flexible chains to $k_B T_s/\epsilon = 1.75$ for stiff chains) as stiffness increases (Table I). The densities of these systems at T_s also drop sharply with increasing k_{bend} over the same range; Table I reports the packing fractions $\phi_s = \phi(T_s)$, where $\phi = \pi\rho/6$ is the usual packing fraction for spherical particles [and $\rho = N_{ch}N/V$ is the monomer number density]. Thus these systems collectively exhibit a wide range of solidification behaviors.

Crystallizing systems exhibit sharp, first-order-transition-like jumps in $\langle Z_{nc}(T) \rangle$ at $T = T_s$. Glass-forming systems exhibit smoothly increasing $\langle Z_{nc}(T) \rangle$ as T decreases, with only slight cusps [discontinuities in $\partial^2 \langle Z_{nc}(T) \rangle / \partial T^2$] at $T = T_s$. [26] Below T_s , $\langle Z_{nc}(T) \rangle$ continues to increase as cooling proceeds, not because of any major structural rearrangements, but simply because systems continue to densify. It is clear that both flexible-chain systems and stiff-chain systems are approximately isostatic at $T = T_s$, i.e. they respectively have $\langle Z_{nc}(T_s) \rangle \simeq \langle Z_{nc}^{iso} \rangle_{flex}$ and $\langle Z_{nc}(T_s) \rangle \simeq \langle Z_{nc}^{iso} \rangle_{stiff}$. It is also clear that intermediate-stiffness systems display intermediate solidification behavior that exhibits a smooth crossover between the flexible-chain and stiff-chain limits.

Refs. [10, 11] reported $\langle Z_{nc}(T_s) \rangle \simeq \langle Z_{nc}^{iso} \rangle_{flex}$ in single-flexible-chain systems. Refs. [11, 12] argued that $\langle Z_{nc}(T_s) \rangle$ should be $\langle Z_{nc}^{iso} \rangle_{flex}$ in bulk glassforming polymeric liquids when chains are fully flexible, and $\langle Z_{nc}^{iso} \rangle_{stiff}$ when chains are infinitely stiff (have holonomic $\theta = \theta_0$ constraints). Panel (b) shows $\langle Z_{nc}(T_s) \rangle$ for all systems as a function of k_{bend} . $\langle Z_{nc}(T_s) \rangle$ is roughly constant for $k_{bend} < \sim \epsilon$, then drops sharply with increasing k_{bend} until the stiff-chain $\langle Z_{nc}(T_s) \rangle \simeq \langle Z_{nc}^{iso} \rangle_{stiff}$ limit is approached as k_{bend} exceeds $\sim 10\epsilon$. The data

in panels (a-b) clearly show that $\langle Z_{nc}(T_s) \rangle \simeq \langle Z_{nc}^{iso} \rangle_{flex}$ also holds true for crystal-forming flexible-chain liquids, and that $\langle Z_{nc}(T_s) \rangle \simeq \langle Z_{nc}^{iso} \rangle_{stiff}$ holds for crystal-forming stiff-chain liquids. They also strongly suggest semiflexible chains' solidification behavior should be describable by a suitably generalized criterion for $\langle Z_{nc}(T_s) \rangle$.

One commonly used measure of chain stiffness that is easily connected to the configurational freedom associated with bond angles is the characteristic ratio $C_\infty = (1 + \langle \cos(\theta) \rangle) / (1 - \langle \cos(\theta) \rangle)$. $C_\infty = 1$ for ideally flexible chains with no excluded volume, ~ 1.7 for $k_{bend} = 0$ chains,[23, 27] and ∞ for $k_{bend} = \infty$ rod-like chains. Thus the variation of C_∞ can be taken as a rough proxy for the slow freezing out of the bond-angular degrees of freedom as chain stiffness increases and/or temperature decreases. While many-body effects can considerably alter C_∞ in bulk systems (e.g. dense liquids at $T = T_s$ or athermal systems at $\phi = \phi_J$ [17, 27]), it is still reasonable to posit that a generalized isostaticity criterion based on C_∞ exists. One postulate is that the *effective* number of holonomic constraints per chain at solidification is

$$n_{constr}^{eff}[C_\infty(T_s)] = (N - 1) + (N - 2)g[C_\infty(T_s)], \quad (7)$$

where $g(C_\infty)$ smoothly increases from 0 to 1 as C_∞ varies from 1 to ∞ . Then a potential generalized isostaticity criterion is

$$\langle Z_{nc}^{iso} \rangle_{gen} = 2N^{-1}(Nd - n_{constr}^{eff}[C_\infty(T_s)]). \quad (8)$$

with n_{constr}^{eff} given by Eq. 7. This formula automatically satisfies $\langle Z_{nc}^{iso} \rangle_{gen} = \langle Z_{nc}^{iso} \rangle_{flex}$ when $C_\infty = 1$ and $\langle Z_{nc}^{iso} \rangle_{gen} = \langle Z_{nc}^{iso} \rangle_{stiff}$ when $C_\infty = \infty$, and thus is consistent with Eqs. 1 and 2. Since it is not clear how to calculate $g(C_\infty)$ “ab initio”, we will attempt to determine a functional form for $g(C_\infty)$ by examining our simulation-generated dataset.

Figure 1(c) shows $\langle Z_{nc}(T_s) \rangle$ for all systems as a function of $C_\infty(T_s)$. Systems with $k_{bend}/\epsilon < \sim 1.5$ [$C_\infty(T_s) < \sim 7$] are apparently in the flexible-chain limit where $g(C_\infty) \simeq 0$ and $\langle Z_{nc}(T_s) \rangle \simeq \langle Z_{nc}^{iso} \rangle_{flex}$. For larger k_{bend} and $C_\infty(T_s)$, the decrease of $\langle Z_{nc}(T_s) \rangle$ with increasing chain stiffness is approximately logarithmic in $C_\infty(T_s)$. Stiff chains with $C_\infty(T_s) \simeq 50$ have $\langle Z_{nc}(T_s) \rangle \simeq \langle Z_{nc}^{iso} \rangle_{stiff}$. The data suggest $g(C_\infty) \sim \ln[C_\infty]$ for $7 < \sim C_\infty < \sim 50$, and that a generalized isostaticity criterion of form

$$\langle Z_{nc}^{iso} \rangle_{gen} = \min \left[\langle Z_{nc}^{iso} \rangle_{flex}, \langle Z_{nc}^{iso} \rangle_{stiff} - b \ln \left(\frac{C_\infty}{C_\infty^{max}} \right) \right] \quad (9)$$

describes the solidification of semiflexible polymers over the full range of C_∞ considered here; as shown in panel (c), the fit of Eq. 9 to the data for $k_{bend}/\epsilon \geq 2\epsilon$ is very good. Note that this range of C_∞ is comparable to the range exhibited by natural polymers, from very flexible ones such as polyethylene to stiff ones such as actin.[13, 14] Very stiff chains with $C_\infty \geq C_\infty^{max} \simeq 10^2$ lie in a

different regime where chains behave as though they were single rigid-rod-like particles rather than polymers,[28, 29] and are not considered here.

The crossover from the flexible to the semiflexible regime (i.e. the crossover between the two functional forms for $\langle Z_{nc}^{iso} \rangle_{gen}$ given in Eq. 9) is a subtle issue. The data in Fig. 1 actually suggests that polymer melts are *very* slightly hypostatic at solidification, to a degree that is nearly independent of chain stiffness. This slight deviation may be related to solidification occurring when iso/hyper-static clusters percolate rather than when $\langle Z_{nc} \rangle = \langle Z_{nc}^{iso} \rangle_{gen}$, [30] but analyses of such clusters in our systems were inconclusive. Alternatively, the deviation may be related to thermal effects including nonperturbative effects of attractive interactions and the shape of the repulsive part of the potential,[31] or many-body phenomena including dimer-interlocking.[32] Such effects are usually subtle and would require intensive analyses that are beyond our present scope. Thus the generalized isostaticity criterion developed here (Eq. 9) can be considered a peer of those proposed in Refs. [1–6] in the sense that while it is neither rigorous nor precise, it can serve as a useful guide.

IV. DISCUSSION AND CONCLUSIONS

The trends illustrated in Fig. 1 strongly suggest that isostaticity is a broadly important concept for improving our understanding of semiflexible polymer solidifica-

tion. The $\ln(C_\infty)$ dependence of $\langle Z_{nc}(T_s) \rangle$ in our thermal systems is also observed in jamming of athermal semiflexible polymers, which have $\langle Z_{nc}(\phi_J) \rangle \simeq a - b \ln(C_\infty)$ in the range $10^1 < \sim C_\infty < \sim 10^2$. [17] This similar functional dependence of monomer coordination at solidification upon C_∞ is present despite the fact that Ref. [17] employed a different angular potential [$U_b = (k_{bend}/2)(\theta - \theta_0)^2$] and varied C_∞ by varying θ_0 rather than k_{bend} . The common behavior supports previous work (e.g. Refs.[9, 11, 12, 16]) suggesting that jamming-related phenomena play a role in controlling polymer melt solidification despite the fact that polymer melts are highly thermal. For example, the well-known increase in T_g with increasing C_∞ in microscopic synthetic polymers,[13, 14] the observed decrease in ϕ_J with C_∞ in athermal polymers,[16, 17] and the data presented herein all form a consistent picture if one accepts the idea that all these trends are dominated by the gradual freezing out of configurational freedom as chain stiffness increases. In conclusion, the accumulated evidence now strongly suggests that C_∞ is an axis on the polymeric counterpart of Liu and Nagel’s jamming-glass phase diagram.[33]

V. ACKNOWLEDGEMENTS

Alessio Zaccone provided helpful discussions. This material is based upon work supported by the National Science Foundation under Grant Nos. DMR-1555242 and DMR-1560090.

-
- [1] H. R. Wendt and F. F. Abraham, Phys. Rev. Lett. **41**, 1244 (1978).
 - [2] A. van Blaaderen and P. Wiltzius, Science **270**, 1177 (1995).
 - [3] E. Corwin, H. M. Jaeger, and S. R. Nagel, Nature **435**, 1075 (2005).
 - [4] T. A. Caswell, Z. Zhang, M. L. Gardel, and S. R. Nagel, Phys. Rev. E **87**, 012303 (2013).
 - [5] C. P. Royall, S. R. Williams, T. Ohtsuka, and H. Tanaka, Nature Mat. **7**, 556 (2008).
 - [6] C. P. Royall and S. R. Williams, Phys. Rep. **560**, 1 (2015).
 - [7] J. C. Maxwell, Philos. Mag. (4th ser.) **27**, 250 (1864).
 - [8] C. S. O’Hern, L. E. Silbert, A. J. Liu, and S. R. Nagel, Phys. Rev. E **68**, 011306 (2003).
 - [9] N. C. Karayiannis and M. Laso, Phys. Rev. Lett. **100**, 050602 (2008).
 - [10] R. S. Hoy and C. S. O’Hern, Soft Matter **8**, 1215 (2012).
 - [11] A. Lappala, A. Zaccone, and E. M. Terentjev, Soft Matter **12**, 7330 (2016).
 - [12] A. Zaccone and E. M. Terentjev, Phys. Rev. Lett. **110**, 178002 (2013).
 - [13] M. Ballauf, Angew. Chem. **28**, 253 (1989).
 - [14] G. Strobl, *The Physics of Polymers* (Springer, 2007).
 - [15] H. T. Nguyen, T. B. Smith, R. S. Hoy, and N. C. Karayiannis, J. Chem. Phys. **143**, 144901 (2015).
 - [16] L.-N. Zou, X. Cheng, M. L. Rivers, H. M. Jaeger, and S. R. Nagel, Science **326**, 408 (2009).
 - [17] R. S. Hoy, Phys. Rev. Lett. **118**, 068002 (2017).
 - [18] R. S. Hoy and N. C. Karayiannis, Phys. Rev. E **88**, 012601 (2013).
 - [19] J. C. Phillips, J. Non-Cryst. Solids **34**, 153 (1979).
 - [20] M. F. Thorpe, J. Non-Cryst. Solids **57**, 355 (1983).
 - [21] M. Micoulaut, Adv. Phys. X **1**, 147 (2016).
 - [22] K. Kremer and G. S. Grest, J. Chem. Phys. **92**, 5057 (1990).
 - [23] R. Auhl, R. Everaers, G. S. Grest, K. Kremer, and S. J. Plimpton, J. Chem. Phys. **119**, 12718 (2003).
 - [24] H. T. Nguyen and R. S. Hoy, Phys. Rev. E **94**, 052502 (2016).
 - [25] S. Plimpton, J. Comp. Phys. **117**, 1 (1995).
 - [26] As in Ref. [15], values of T_g were determined by locating the jump in packing fraction $\phi(T)$ for crystallizing systems, or the intersection of low- T and high- T linear fits to $\phi(T)$ for glassforming systems.
 - [27] K. Foteinopoulou, N. C. Karayiannis, M. Laso, M. Kröger, and M. L. Mansfield, Phys. Rev. Lett. **101**, 265702 (2008).
 - [28] A. V. Kyrylyuk and A. P. Philipse, Phys. Status Solidi A **208**, 2299 (2011).
 - [29] C. P. Broedersz, X. Mao, T. C. Lubensky, and F. C. Mackintosh, Nature Phys. **7**, 983 (2011).

- [30] G. Lois and C. S. O'Hern, Phys. Rev. Lett. **100**, 028001 (2008).
- [31] L. Berthier and G. Tarjus, Phys. Rev. Lett. **102**, 170601 (2009).
- [32] C. F. Schreck, N. Xu, and C. S. O'Hern, Soft Matt. **6**, 2960 (2010).
- [33] A. J. Liu and S. R. Nagel, Nature **396**, 21 (1998).